



**HAL**  
open science

## Simulation Study of the Origin of Ge High Speed Photodetector Degradation

B. Arunachalam, J.-E. Broquin, Quentin Rafhay, D. Roy, A. Kaminski

► **To cite this version:**

B. Arunachalam, J.-E. Broquin, Quentin Rafhay, D. Roy, A. Kaminski. Simulation Study of the Origin of Ge High Speed Photodetector Degradation. 2021 IEEE International Reliability Physics Symposium (IRPS), Mar 2021, Monterey, France. pp.1-4, 10.1109/IRPS46558.2021.9405211 . hal-04742858

**HAL Id: hal-04742858**

**<https://hal.science/hal-04742858v1>**

Submitted on 18 Oct 2024

**HAL** is a multi-disciplinary open access archive for the deposit and dissemination of scientific research documents, whether they are published or not. The documents may come from teaching and research institutions in France or abroad, or from public or private research centers.

L'archive ouverte pluridisciplinaire **HAL**, est destinée au dépôt et à la diffusion de documents scientifiques de niveau recherche, publiés ou non, émanant des établissements d'enseignement et de recherche français ou étrangers, des laboratoires publics ou privés.

# Simulation study of the origin of Ge High Speed Photodetector degradation

B. Arunachalam, Q. Rafhay, A. Kaminski, J.-E. Broquin

Université Grenoble Alpes, CNRS, Grenoble INP, IMEP-LAHC, 38000 Grenoble, France, Université Savoie Mont Blanc, IMEP-LAHC, 74000 Annecy, France  
balraj.arunachalam@grenoble-inp.fr

D. Roy

<sup>1</sup>STMICROELECTRONICS, 850 rue Jean Monnet, 38926 Crolles cedex, France

**Abstract**—The reliability of Si photonics and optoelectronic devices is emerging as a major new topic. By using TCAD simulations, this work investigates the microscopic origins of the Ge High Speed Photodetector (HSPD) performance losses during stress obtained in [1]. It confirms the key roles of the carrier lifetime degradation on both dark current increase and photonics current decrease, which could be triggered by surface recombination (SR), especially at the Buried Oxide (BOX). Other sources of degradation are studied, as fixed charges in the SiO<sub>2</sub> passivation layer and interface state (D<sub>it</sub>).

## I. INTRODUCTION

Optoelectronic devices are one of the building blocks of optical telecommunications and Si photonics. Up to now, the only reliability protocols for telecom applications are the Telcordia ones [2], which implies very long pass/fail test (2000h). As no physical understanding of the degradation of Si photonics devices has been reached yet, these tests are still the reference one. [1] and [3] have however recently experimentally demonstrated that HSPD are prone to significant dark current and responsivity degradation with voltage stresses and temperature. Using a simple model, these degradations have been attributed in [1] to degradation of the carrier lifetime, inducing strong carrier recombination. The aim of this work is to investigate the HSPD reliability using Sentaurus TCAD. The impact of carrier lifetime ( $\tau$ ) will be at first studied, followed by the roles of different transport mechanisms, which could occur in these p-i-n diodes. The influence of SR on the  $I_{\text{dark}}$  will be detailed. Finally, other sources of degradation like fixed charges and  $D_{\text{it}}$  will be included.

## II. IMPACT OF CARRIER LIFETIME

The studied device is built on a SOI wafer, whose Si film is etched to form optical waveguide, along which the HSPD is placed [4]. The Transmission electron microscopy (TEM) image of the HSPD is given in fig. 1. In fig 2 are given the two architectures studied in this work. A first simple pseudo 1D structure is studied to match the 1D model of [1]. The second 2D structure is designed to mimic the geometry of fig. 1. The optical generation rate is constant in the whole device and equal to  $6.75 \cdot 10^{25} \text{ cm}^{-3}\text{s}^{-1}$ . The results obtained in [1] will be checked at first on the pseudo 1D structure including only SRH recombination. By varying the carrier lifetime  $\tau$ , dark I-V (fig. 3) and illuminated (fig. 5) characteristics are obtained. It can be seen that the dark current increases with decrease in  $\tau$ , due to the increase of carrier recombination, or equivalently, the decrease of carrier diffusion length (fig. 4). The raw illuminated I-V curves are less straight forward to interpret

(fig. 5). The decrease of  $\tau$  induces at first a decrease of the light current, which then increases again for very small  $\tau$  (fig. 6). However, the responsivity is function of the photonics current defined by  $I_{\text{phot}} = I_{\text{light}} - I_{\text{dark}}$ . When plotting  $I_{\text{phot}}$  vs  $\tau$  (fig 6) the trend is monotonic and fully confirms the results obtained in [1].

## III. TRANSPORT MECHANISMS AND RECOMBINATIONS

The impact of different transport mechanisms is shown in fig. 7, where SRH dominated  $I_{\text{dark}}$  is compared to the SRH / Band-To-Band (BTB) and BTB / Trap Assisted Tunneling (TAT). In Sentaurus, TAT is treated as a field enhancement of SRH [5], which explains the common trends at low voltage. High voltages are always dominated by BTB. On fig. 8 is compared the pseudo 1D and 2D structure, showing a strong increase of  $I_{\text{dark}}$  with geometric variation. All other simulations have been carried out with the 2D structure. On fig. 9 is added the impact of the SR at the interface of a surrounding passivation layer (fig. 11(a)). It can be seen that the increase of the surface recombination velocity (SRV) leads to increase of  $I_{\text{dark}}$ , as in the case of the decrease of  $\tau$ . When excluding all other recombination, variation of SRV from 0 to  $10^7 \text{ cm/s}$  can give variation of current over 6 orders of magnitude (fig. 10). SR can therefore explain the degradation of  $I_{\text{dark}}$  obtained in [1]. On fig. 12 is compared different placement of SR, either all around the device (fig. 11(a)), or only on top (fig. 11(b)). This shows that the top part plays a marginal role, and that the BOX section leads to significant degradation, highlighting the necessity to correctly passivate this interface.

## IV. OTHER SOURCES OF DEGRADATION

Other sources of potential degradation have been included in the simulation to estimate their impact: negative (fig. 13) and positive (fig. 14) fixed charge in a surrounding oxide, its impact on different transport mechanisms (fig. 15), the role of its placement (fig. 16 and 17) and interface states (fig. 18). None of them has been found to significantly degrade the dark current.

## V. CONCLUSIONS

These simulation results hence confirm that the dark current and photonic current degradation observed in [1] are indeed explained by lifetime collapse during stress, potentially triggered by the increase of surface recombination. They imply that great care should be taken with the passivation of the encapsulation layers, especially at the bottom of the device. Additional experimental work will be required in the future to study the dynamic increase of surface recombination.

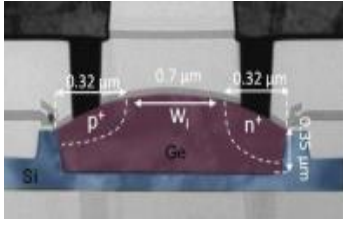


Fig. 1: TEM of the HSPD.  
 $N_d = 6 \cdot 10^{18} \text{ cm}^{-3}$ ,  $N_a = 3 \cdot 10^{19} \text{ cm}^{-3}$

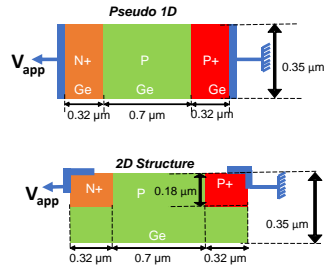


Fig. 2: Simulated geometries of the pseudo 1D and 2D structure.

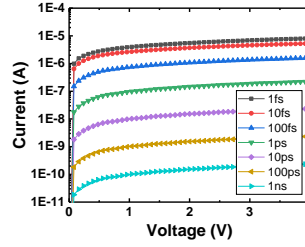


Fig. 3:  $I_{\text{dark}}$  vs V for different lifetime of the Ge.

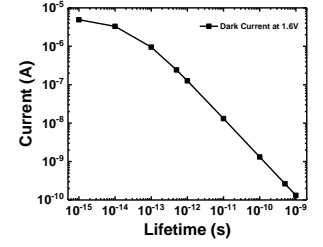


Fig. 4:  $I_{\text{dark}}$  vs  $\tau$  reproducing the degradation observed in [1]

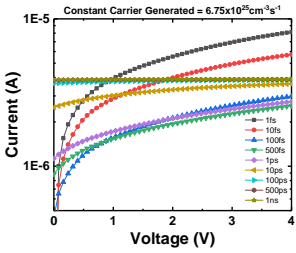


Fig. 5:  $I_{\text{light}}$  vs V for different  $\tau$  for a constant optical generation rate in the HSPD

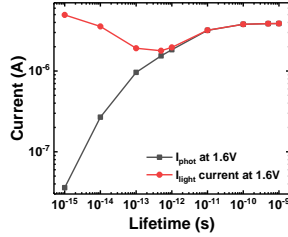


Fig. 6:  $I_{\text{light}}$  and  $I_{\text{phot}}$  vs  $\tau$  showing that a strong part of  $I_{\text{light}}$  is due to  $I_{\text{dark}}$  for very small  $\tau$

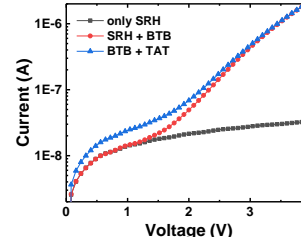


Fig. 7: Impact of different transport mechanisms on the I-V of the pseudo 1D geometry

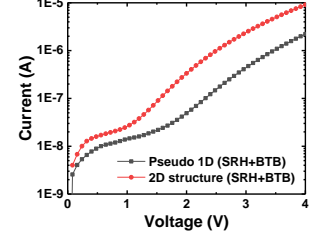


Fig. 8: Impact of the geometry on the  $I_{\text{dark}}$  of the HSPD

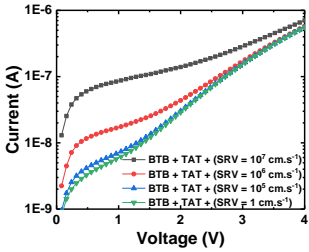


Fig. 9:  $I_{\text{dark}}$  vs V including all mechanisms for different values of SRV (2D geometry)

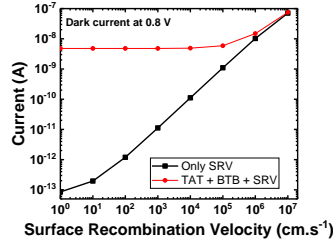


Fig. 10: Increase of  $I_{\text{dark}}$  with SRV when excluding all mechanisms, or including them

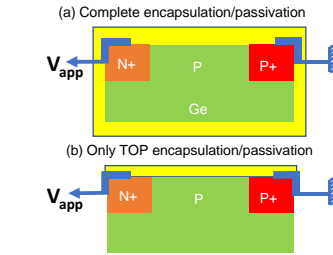


Fig. 11: Scheme of the SRV placement (a) all around or (b) only at the top

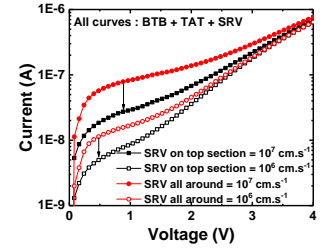


Fig. 12:  $I_{\text{dark}}$  vs V for different placement of the SRV (fig. 11) and two values of SRV.

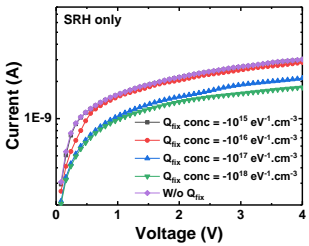


Fig. 13:  $I_{\text{dark}}$  vs V for different concentration of negative  $Q_{\text{fix}}$

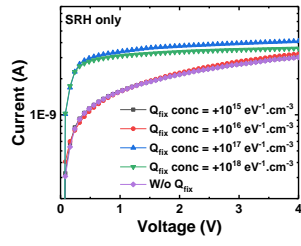


Fig. 14:  $I_{\text{dark}}$  vs V for different concentration of positive  $Q_{\text{fix}}$

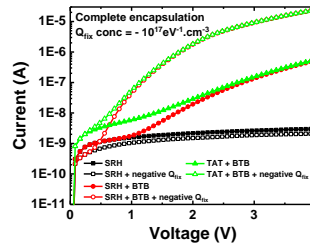


Fig. 15: Impact of  $Q_{\text{fix}}$  on the  $I_{\text{dark}}$  vs V including different transport mechanisms

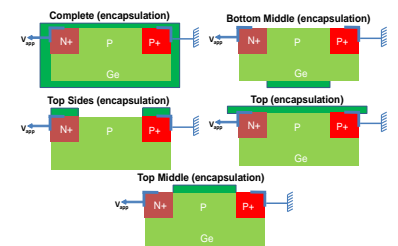


Fig. 16: Scheme of the  $Q_{\text{fix}}$  placement around the device

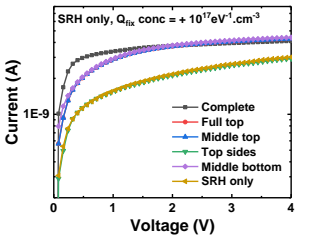


Fig. 17: Impact of the  $Q_{\text{fix}}$  placement around the device on  $I_{\text{dark}}$

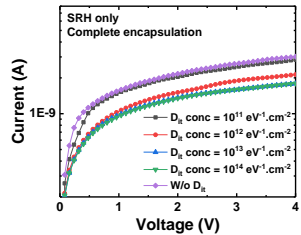


Fig. 18:  $I_{\text{dark}}$  vs V for different interface state densities

References:

- [1] F. Sy *et al*, IEEE IRPS 2019
- [2] TELCORDIA GR-468-CORE Generic Reliability Assurance Requirements for Optoelectronic Devices Used in Telecommunication Equipment
- [3] A. Leśniewska *et al.*, IEEE IRPS 2019
- [4] F. Boeuf *et al.*, IEEE IEDM 2013
- [5] Sentaurus™ Device User, 2019, Sentaurus version used: 2016

Acknowledgements:

This work has been funded by the ICPEI Nano2022 FiabPhSi project